Electronic Supplementary Material (ESI) for Chemical Communications.

Supplementary Information

Tuning the phase separation of PEDOT:PSS affords efficient lead-free perovskite solar cells

Hui Zhang,[a] Shurong Wang,[a] Huanhuan Yao,[a] Zhiyue Tang,[a] Liming Ding,[b] Feng Hao[a*]

[a] *School of Materials and Energy, University of Electronic Science and Technology of China, Chengdu, 611731, China*

[b] *Center for Excellence in Nanoscience (CAS), Key Laboratory of Nanosystem and Hierarchical Fabrication (CAS), National Center for Nanoscience and Technology, Beijing, 100190, China*

*Corresponding authors.

E-mail addresses: haofeng@uestc.edu.cn

Experimental section

Materials

Indium tin oxide (ITO), Ethanol (EtOH), phenethylammonium Iodide (PEAI) and silver (Ag) were separately purchased from Advanced Election Technology, Reagent, Trilllion Metals and Xi'an Polymer Light Technology Corp. Isopropanol (IPA), Tin (II) iodide (SnI_2) and bathocuproine (BCP) were purchased from Adamas-beta. Formamidinium iodide (FAI) and large cationic salt (Methylammonium bromide, MABr) is bought from GreatCell. N, N-dimethylformamide (DMF), polar organic solvent dimethyl sulfoxide (DMSO), solid Sn^0 powder and tin fluoride (SnF_2) is purchased from Sigma-Aldrich.

Device preparation

The ITO substrates, after rinsed by deionized water, then cleaned with ethanol and acetone, and finally stored in isopropyl alcohol. Afterwards, the ITO was dried for 13 mins with a stream of nitrogen gas in UV ozone. Then, the substrate needed to be properly cooled, immediately spin coated at 4100 rpm for 55 s with PEDOT:PSS (annealed at 135 °C for 18 mins). 8 mg/ml ammonium carbamate dissolved in PEDOT was spin-coated with the same conditions, and annealed at 118 °C for 13 mins. After that, precursor solution is prepared by the component of $FA_{0.75}MA_{0.25}SnI_{2.75}Br_{0.25}$ with excess 10% SnF_2 and 6% Sn^0 in the solvent, where the volume ratio of DMF and DMSO is 4:1. Precursor, after stirring for 7 h, then mixed for 1h with 15% PEAI and 4% Sn^0 together. Tin-based perovskite precursors should be spread over the PEDOT:PSS substrate at the speed of 8000 rpm for 60 s and extracted with a rapid drop of 170 µL CB at 52 s. Then the substrate was placed on a hot table at 85 °C for 12 mins to anneal. 45 µL C_{60}-ETPA[1] (22 g L^{-1} in CB) together with the 95 µL BCP (0.5 g L^{-1} in IPA) needed to be spin-coated on the substrate in turn and annealed at 75 °C for 12 mins respectively. The respective spin coating conditions are 2000 rpm 30 s and 6000 rpm 30 s. The last procedure is to slowly steam 110 nm silver in a high temperature vaporizer onto the accomplished film.

Device characterization

The analysis data of X-ray photoelectron spectroscopy (XPS), infrared data, UV-vis absorption and X-ray diffraction (XRD) instrument were respectively obtained from AXIS UltraDLD instrument, Fourier transform infrared spectroscopy (FTIR, Bruker, UV-2600 (Shimadzu) and MiniFlex 600 (Rigaku). Current density-voltage (*J-V*) curves were obtained from a 2400 source meter (Keithley). The typical measurement atmosphere was in a standard AM 1.5 G that is 100 mW cm^{-2}. The integrated current was measured by QE-R (Enlitech). The steady photoluminescence (PL) spectroscopy was tested utilizing Fluo Time 300 (PicoQuant), which is the same with time-resolved photoluminescence (TRPL). The carrier dynamics of transient photovoltage (TPV),

impedance spectroscopy (IS), and transient photocurrent (TPC) along with open-circuit voltage decay (OCVD) were strictly monitored from Piaos 4.0 system (FLUXiM). The conducting area of the solar cells was 0.096 cm^2.

1. Equation (1) was employed to model the σ of the PEDOT:PSS:[2, 3]

$$I = \sigma SVd^{-1} \quad (1)$$

where *S* and *d* respectively correspond to the area and thickness of film.

2. ε_r is calculated from the change in displacement current:[4-7]

$$\varepsilon_r = \frac{j_{disp} \cdot d}{A \cdot \varepsilon_0} \quad (2)$$

where *A*、 *d* and ε_0 correspond to the ramp rate, perovskite layer thickness and the relative dielectric constant, respectively.

3. μ can be calculated by the equation:[8]

$$J = \frac{9}{8}\mu\varepsilon\varepsilon_0\frac{V^2}{d^3} \quad (3)$$

where ε_0, ε, and d mean the relative permittivity, dielectric constant, and film thickness, respectively.

4. The differential capacitance (*C*) is calculated from Δ*Q* and ΔV_{oc}:[9, 10]

$$C = \frac{\Delta Q}{\Delta V_{oc}} \quad (4)$$

where Δ*Q* is the short-circuit photogenerated charge integrated from the TPC results, and the ΔV_{oc} under different light intensity can be obtained from the OCVD test results.

5. DOS can be derived from the capacitance using the equation: [9,10]

$$DOS = \frac{C}{Le^2} \quad (5)$$

where *C* is the chemical capacitance, *L* is the thickness of perovskite film, *e* is the elementary charge.

6. The carrier concentration (*n*) can be modeled as follow:[11]

$$n = \frac{1}{ALe}\int_0^{V_{oc}} CdV \quad (6)$$

where *A*, *L* and *e* corresponds to the device area, the thickness of perovskite film and the elementary charge, respectively.

7. The charge transport lifetime (τ_{tr}) and charge recombination lifetime (τ_{rec}) were calculated as follows:[12]

$$\tau_{tr} = \frac{1}{2\pi f_{IMPS}} \quad (7)$$

$$\tau_{rec} = \frac{1}{2\pi f_{IMVS}} \quad (8)$$

where f_{IMVS} are the frequencies at which the imaginary part is minimum and f_{IMPS} are the frequencies at which the imaginary part is maximum as shown in Fig. S12.

8. The carrier collection efficiency (η) can be then modeled by equation:[12]

$$\eta = 1 - \frac{\tau_{tr}}{\tau_{rec}} \quad (9)$$

9. The carrier diffusion coefficient (D) and diffusion length (L_D) of different devices is according to the equations:[12]

$$D = \frac{L^2}{2.35\tau_{tr}} \quad (10)$$

$$L_D = \sqrt{D\tau_{rec}} \quad (11)$$

where the L is the thickness of perovskite film.

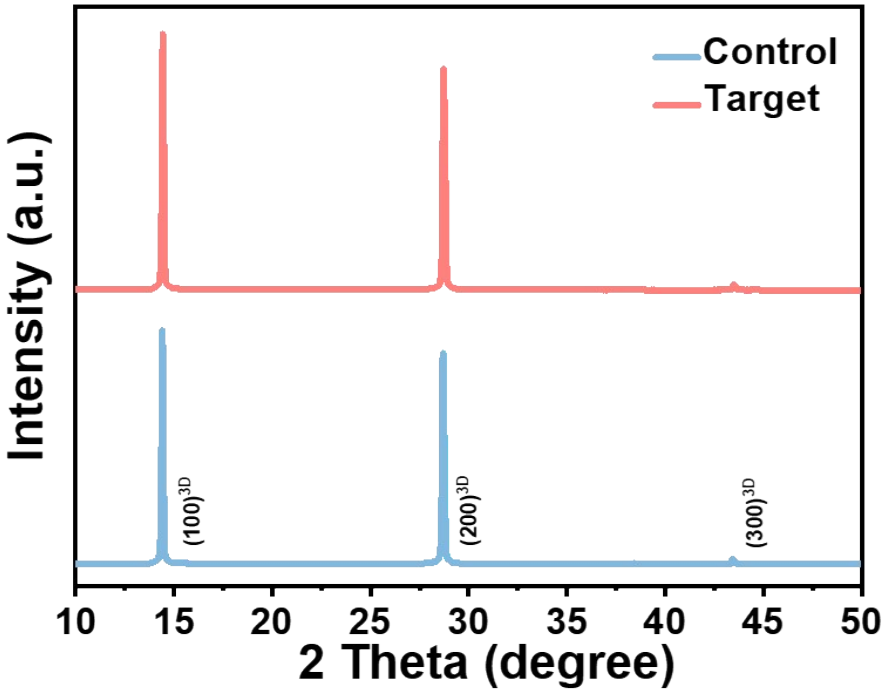

Fig. S1. The XRD patterns of the control and the target perovskite films.

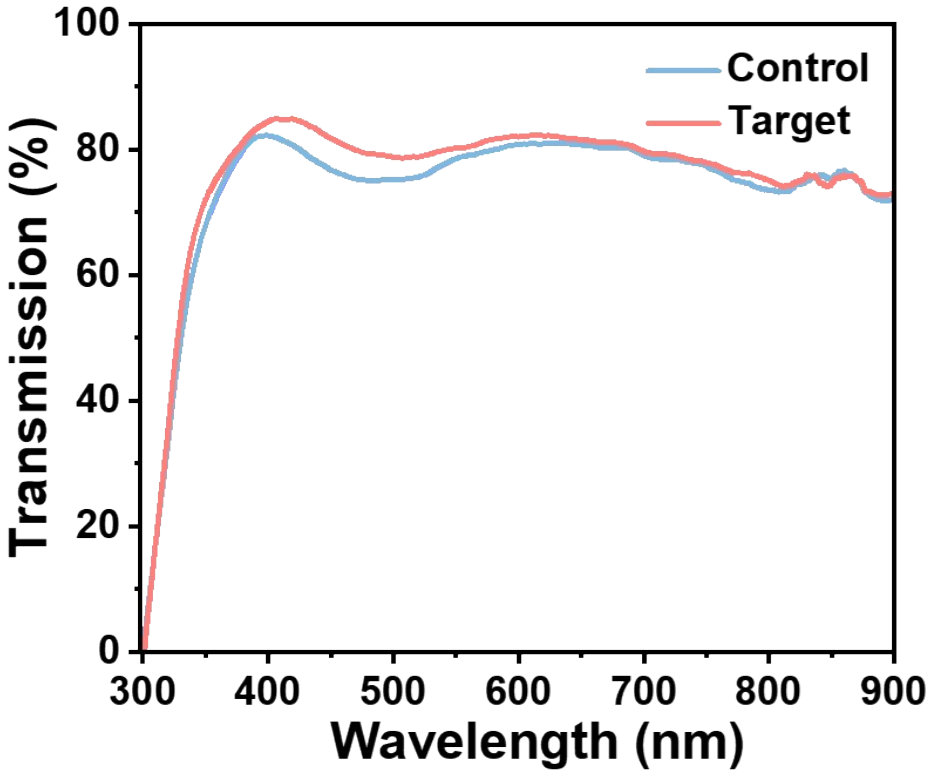

Fig. S2. The transmission spectra for the control and target PEDOT:PSS films.

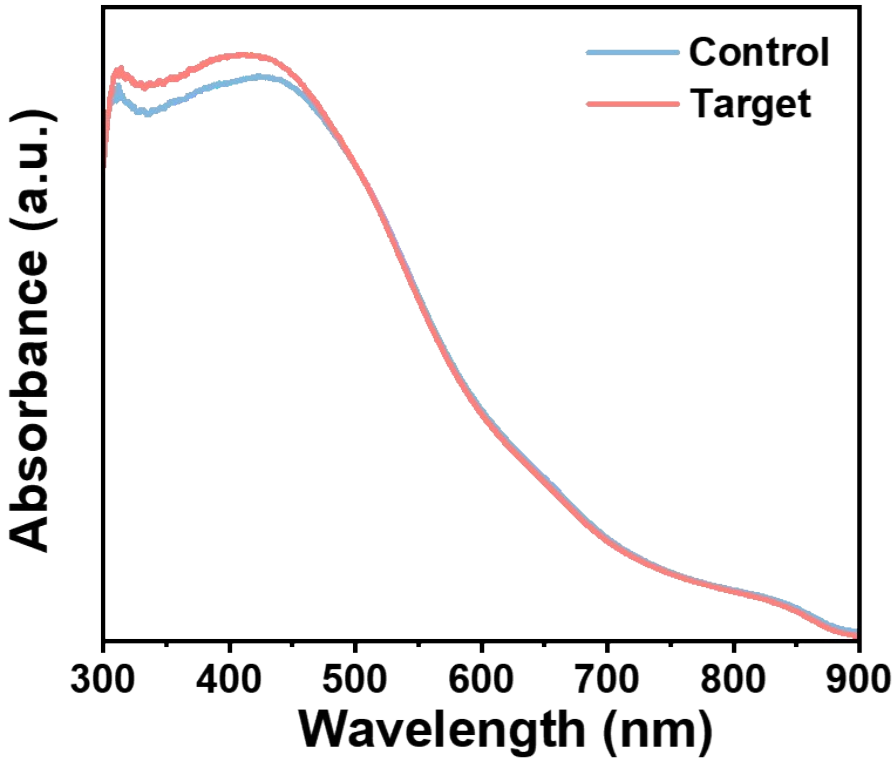

Fig. S3. The Ultraviolet–visible spectroscopy (UV-vis) curves for the control and target perovskite films.

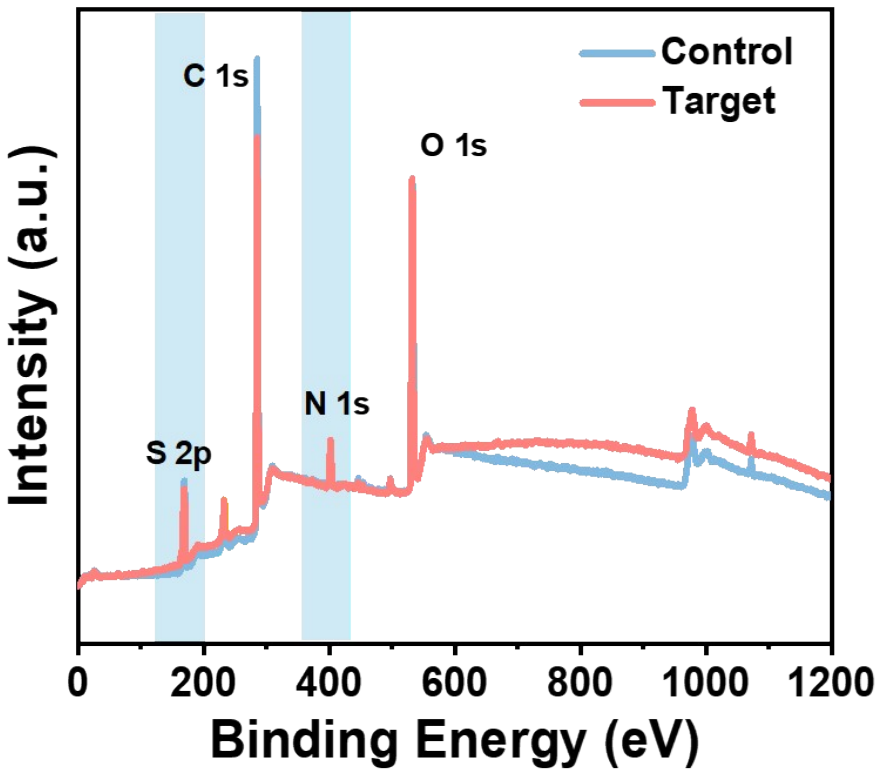

Fig. S4. The wide XPS spectrum of the control film and target film.

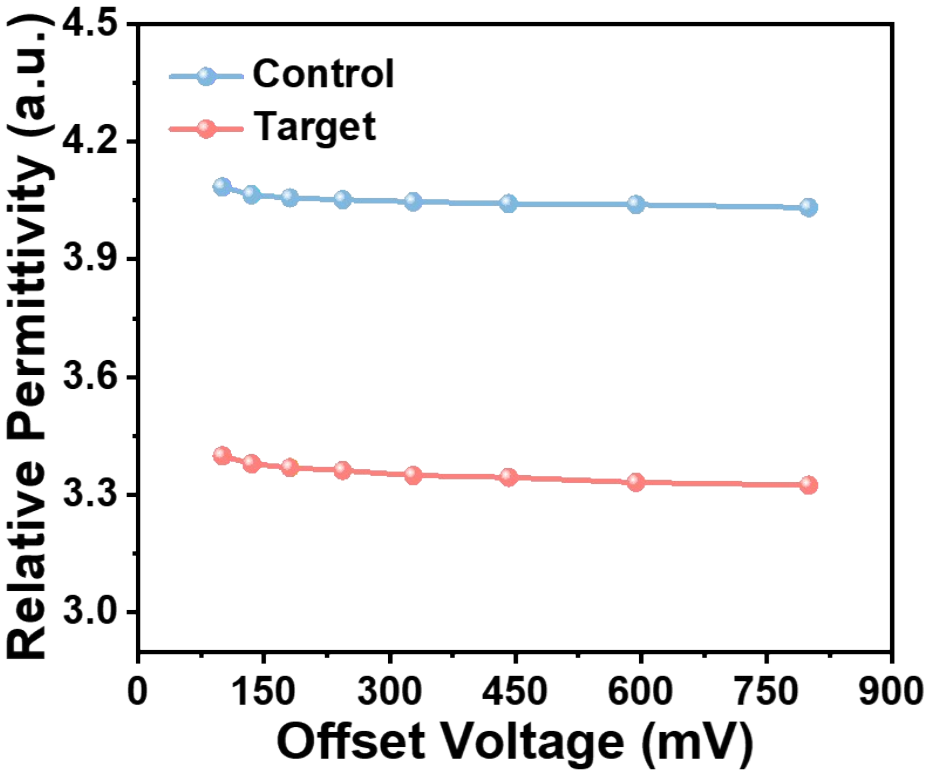

Fig. S5. Relative permittivity values of the control and target devices.

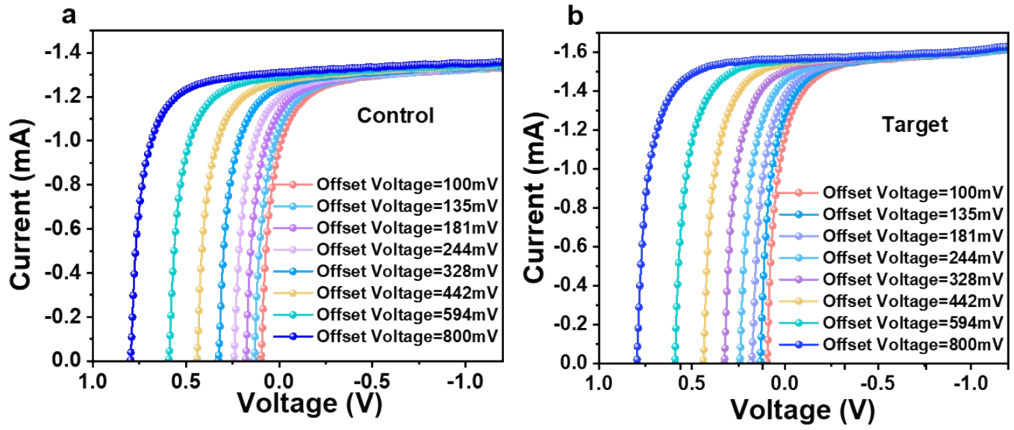

Fig. S6. The Dark-CELIV curves of (a) the control and (b) the target devices.

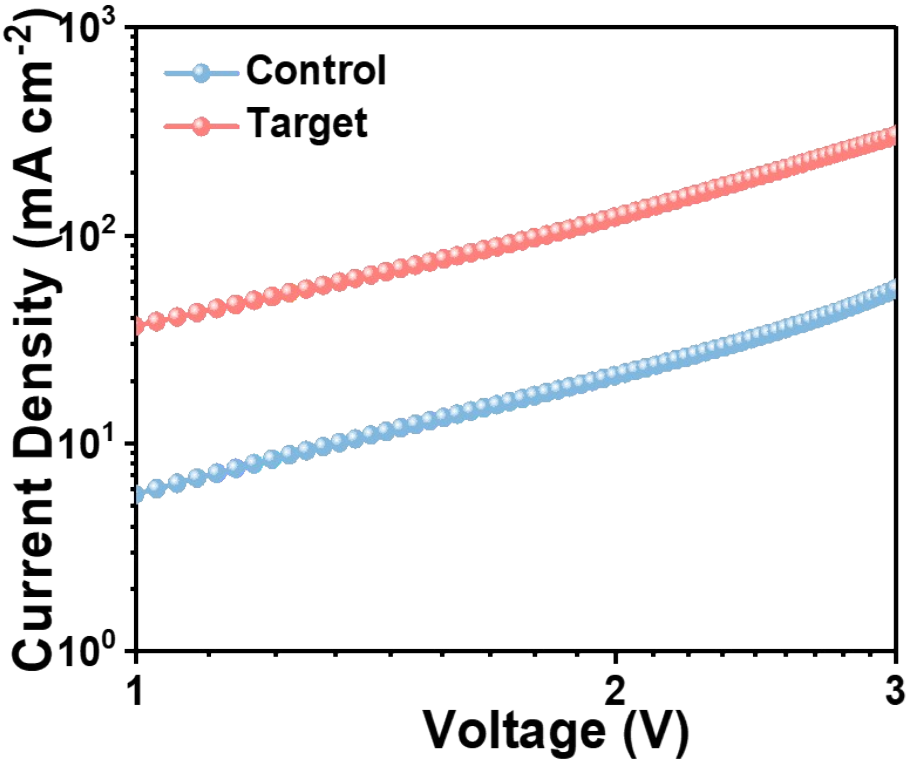

Fig. S7. SCLC plots of hole-only devices made of ITO/PEDOT:PSS/Spiro-OMeTAD/Ag.

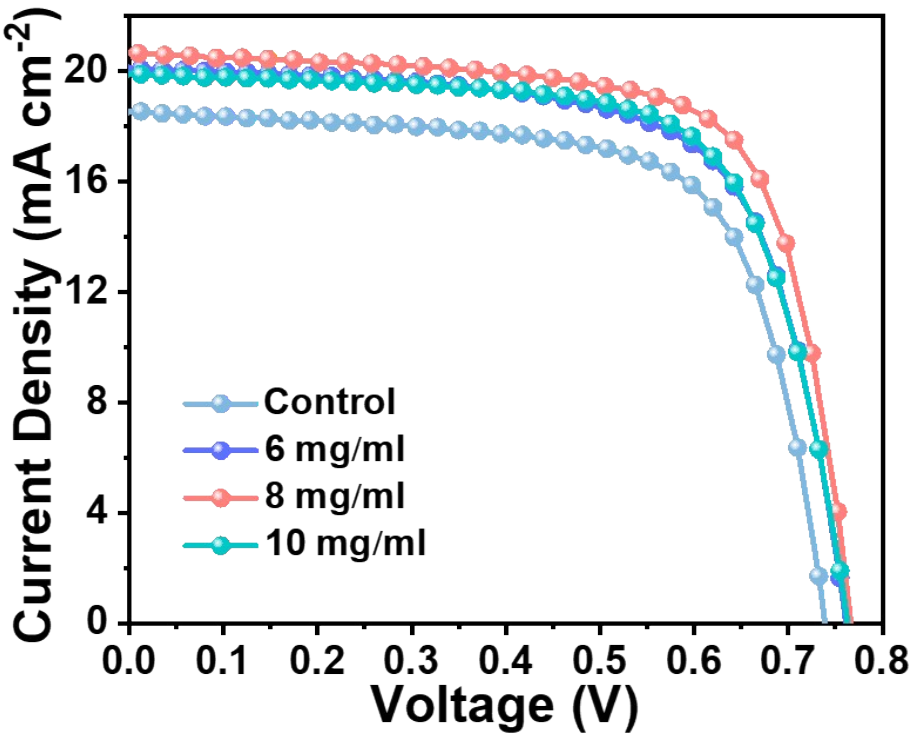

Fig. S8. *J-V* curves for the TPSCs with different AC concentrations.

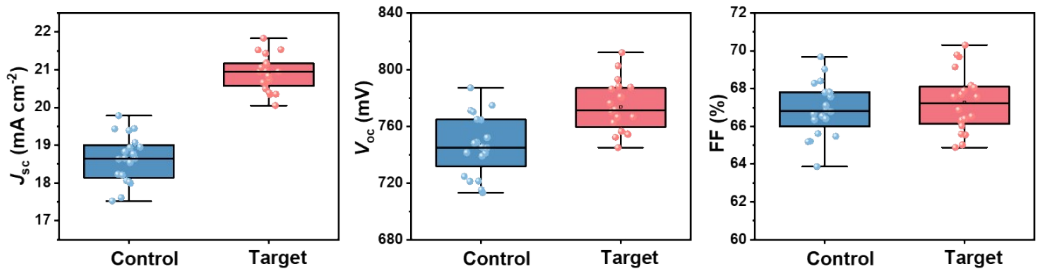

Fig. S9 Histogram of (a) J_{sc} and (b) V_{oc} and (c) FF for a batch of 20 independent devices.

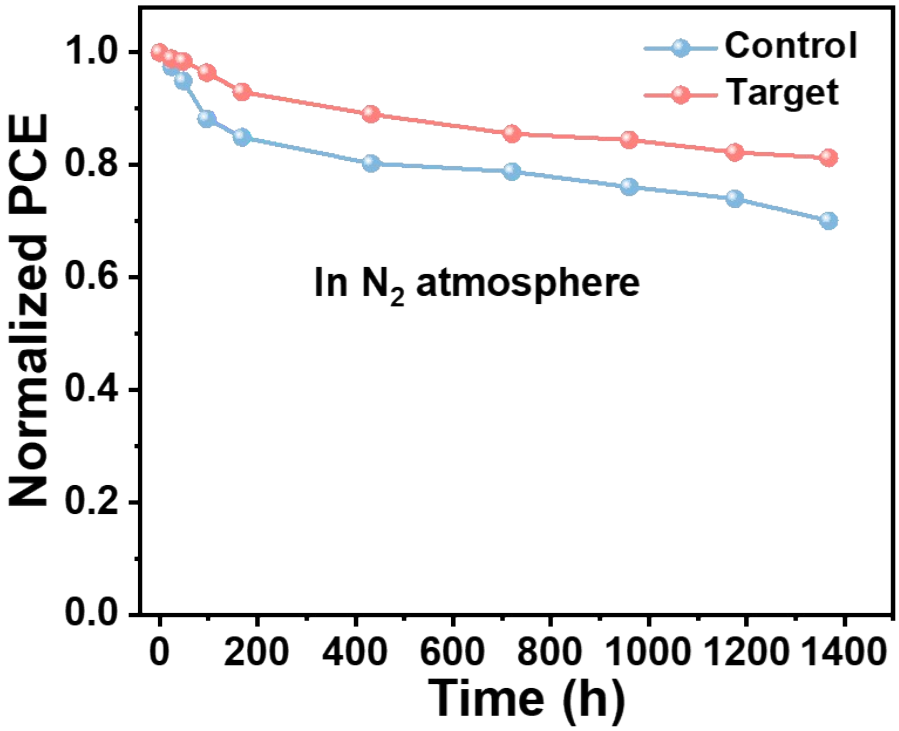

Fig. S10. The stability test of control and target TPSCs.

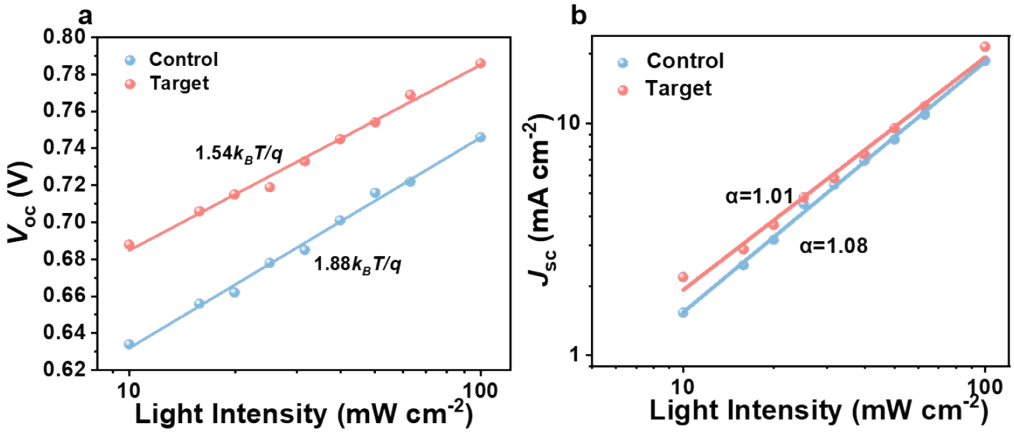

Fig. S11. The light dependence curves of (a) V_{oc} and (b) J_{sc} for the control and target devices.

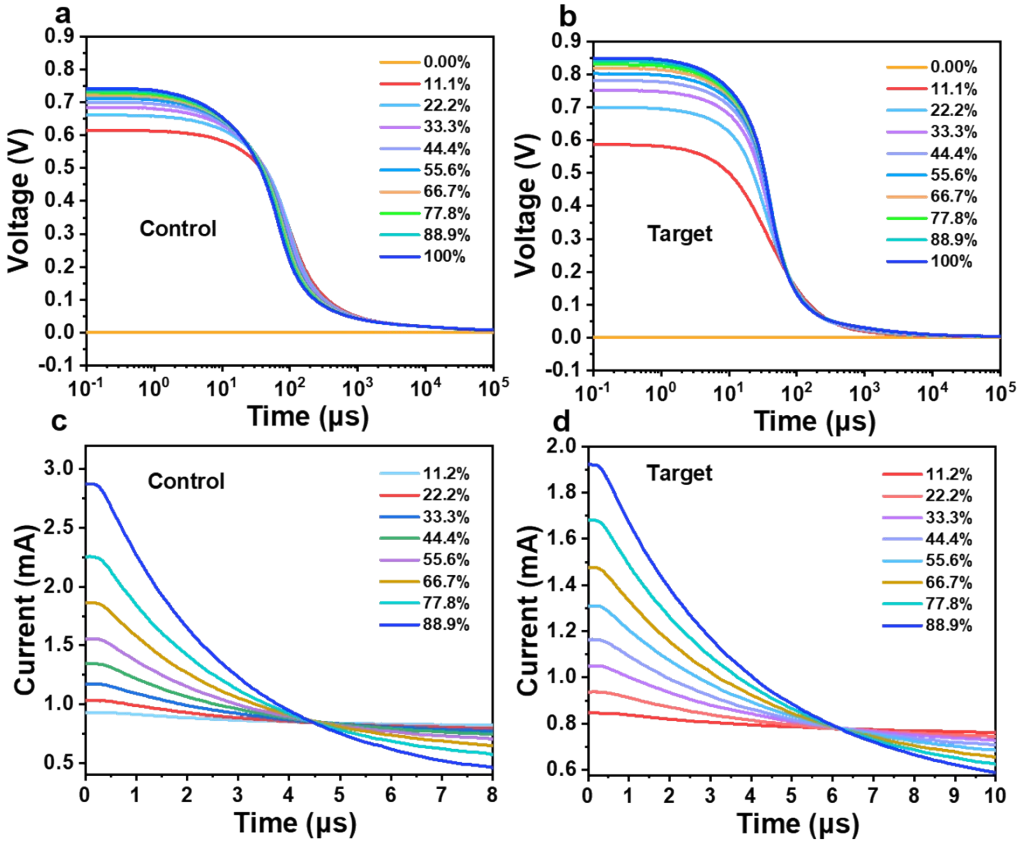

Fig. S12. The OCVD curves for (a) control and (b) target devices, and the TPC curves for (c) control and (d) target devices.

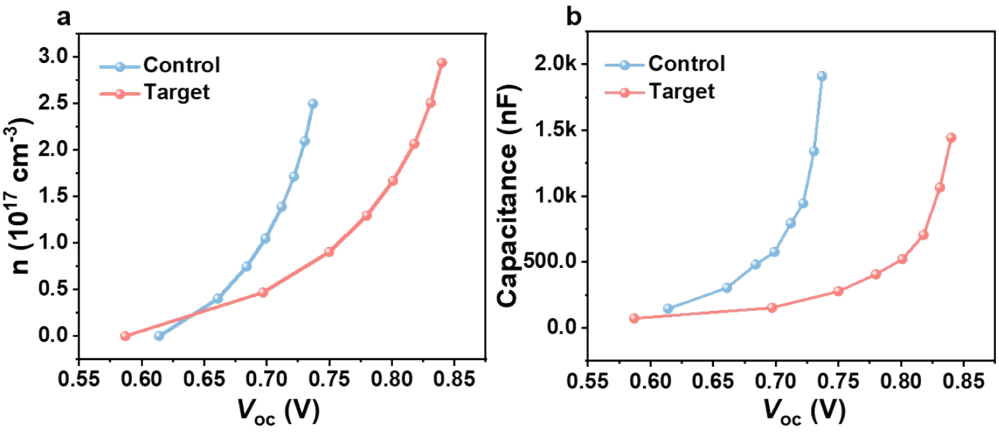

Fig. S13. (a) *C-V* and (b) the carrier concentration in the bandgap for control and target devices from TPC and OCVD data.

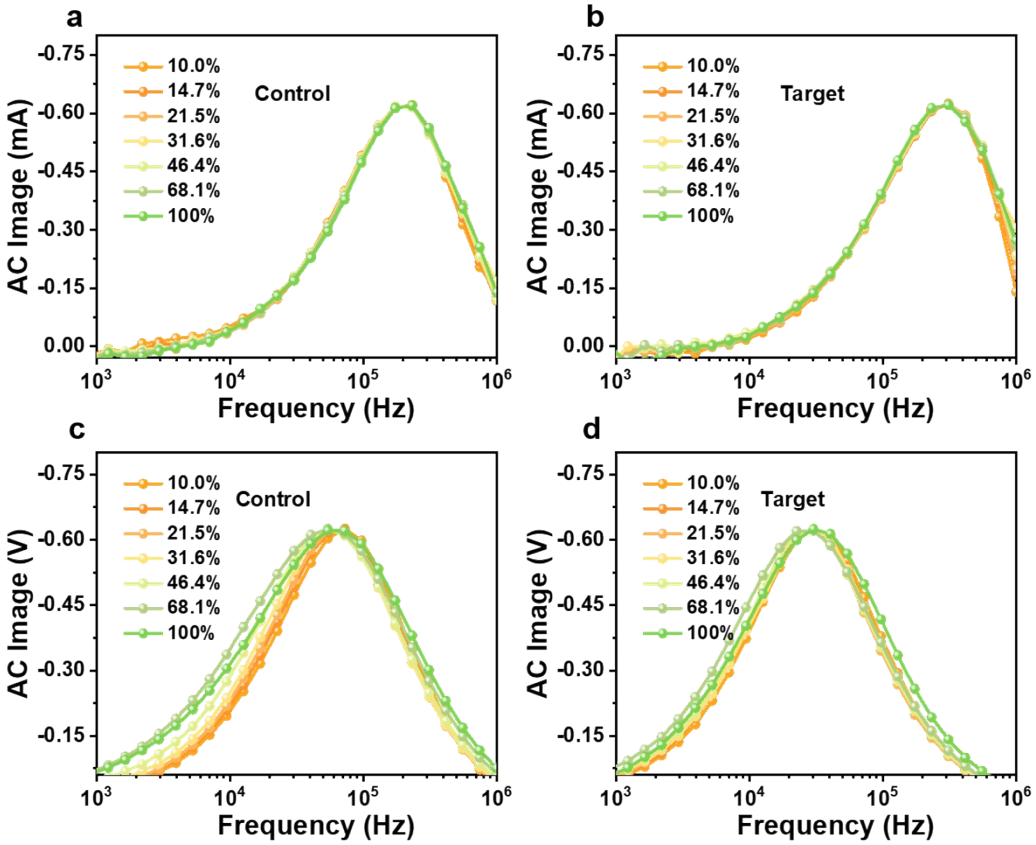

Fig. S14. The intensity-modulated photovoltage spectra (IMPS) curves for (a) control and (b) target devices, the intensity-modulated photocurrent spectra (IMVS) curves for (c) control and (d) target devices.

Table S1. The calculated relative dielectric constant for the control device.

Offset voltage (mV)	C_{disp} (mA)	J_{disp} (A•m^{-2})	ε_r
100	-1.612	167.917	4.032
135	-1.615	168.229	4.039
181	-1.616	168.333	4.042
244	-1.618	168.542	4.047
328	-1.62	168.75	4.052
442	-1.622	168.958	4.057
594	-1.625	169.271	4.064
800	-1.633	170.104	4.084

Table S2. The calculated relative dielectric constant for the target device.

Offset voltage (mV)	C_{disp} (mA)	J_{disp} (A•m^{-2})	ε_r
100	-1.329	138.438	3.324
135	-1.332	138.75	3.332
181	-1.337	139.271	3.344
244	-1.339	139.479	3.349
328	-1.344	140.000	3.362
442	-1.347	140.313	3.369
594	-1.351	140.729	3.379
800	-1.359	141.563	3.399

Table S3. The detailed photovoltaic performance for TPSCs with different concentration of AC.

	V_{oc} (mV)	J_{sc} (mA cm^{-2})	FF (%)	PCE (%)
Control	739	18.53	69.17	9.48
6 mg mL^{-1}	761	20.11	67.80	10.38
8 mg mL^{-1}	766	20.66	71.01	11.24
10 mg mL^{-1}	763	19.90	69.40	10.54

Table S4. The calculated DOS for the control device.

Light intensity	V_{oc} (V)	ΔV_{oc} (V)	Q (nC)	C (nF)	DOS (10^{17} cm^{-3} eV^{-1})
11.1%	0.614	0.047	6.816	145.021	5.547
22.2%	0.661	0.023	6.952	302.261	11.561
33.3%	0.684	0.015	7.195	479.667	18.347
44.4%	0.699	0.013	7.478	575.231	22.002
55.6%	0.712	0.010	7.779	793.776	30.361
66.7%	0.722	0.009	8.211	943.793	36.099
77.8%	0.731	0.006	8.717	1341.077	51.295
88.9%	0.737	0.005	9.552	1910.400	73.070
100%	0.742	0	0	/	/

Table S5. The calculated DOS for the target device.

Light intensity	V_{oc} (V)	ΔV_{oc} (V)	Q (nC)	C (nF)	DOS (10^{17} cm^{-3} eV^{-1})
11.1%	0.587	0.110	7.85	71.364	2.730
22.2%	0.697	0.053	8.046	151.811	5.807
33.3%	0.750	0.030	8.313	277.100	10.599
44.4%	0.780	0.021	8.536	406.476	15.547
55.6%	0.801	0.017	8.853	520.765	19.919
66.7%	0.818	0.013	9.165	705.000	26.965
77.8%	0.831	0.009	9.585	1065.000	40.735
88.9%	0.840	0.007	10.104	1443.429	55.209
100%	0.847	0	0	/	/

Table S6. The calculated *n* for the control and target devices.

	V_{oc} (V)	Integration of C-V_{oc}	n (10^{17} cm^{-3})		V_{oc} (V)	Integration of C-V_{oc}	n (10^{17} cm^{-3})
Control	0.614	0	0	**Target**	0.587	0	0
	0.661	10.511	0.402		0.697	12.275	0.470
	0.684	19.500	0.746		0.750	23.642	0.904
	0.699	27.415	1.049		0.780	33.894	1.296
	0.712	36.314	1.389		0.801	43.630	1.669
	0.722	44.828	1.715		0.818	54.049	2.067
	0.731	54.767	2.095		0.831	65.554	2.507
	0.737	65.334	2.499		0.840	76.842	2.939
	0.742	/	/		0.847	0	0

Table S7. Parameters of the EIS analysis for the control and target devices.

	R_s (Ω)	R_{rec} (kΩ)	C (nF)
Control	7.70	1.12	9.21
Target	4.30	8.34	9.46

Table S8. Diffusion coefficient and length of the control and target devices.

	τ_{tr} (μs)	τ_{rec} (μs)	η (%)	D (nm²/μs)	L_D (nm)
Control	0.78	2.89	72.90	$1.58*10^5$	213.5
Target	0.51	4.89	89.61	$2.41*10^5$	343.4

Table S9. Fitted parameters of the TRPL decays of the control and target perovskite films.

	A_1 (%)	τ_1 (ns)	A_2 (%)	τ_2 (ns)	τ_{avg} (ns)
Control	86.49	13.56	13.51	29.72	17.68
Target	96.16	9.01	3.84	19.16	9.80

References

1. C. Wu, W. Zhu, S. Wang, Z. Cao, L. Ding and F. Hao, *Chem. Commun.*, 2022, **58**, 13007-13010.
2. A. Wang, Z. Cao, J. Wang, S. Wang, C. Li, N. Li, L. Xie, Y. Xiang, T. Li, X. Niu, L. Ding and F. Hao, *J. Energy Chem.*, 2020, **48**, 426-434.
3. Z. Y. Cao, S. R. Wang, W. K. Zhu, L. M. Ding and F. Hao, *Sol. RRL*, 2022, **2200889**, 1-7.
4. M. Neukom, S. Zuefle, S. Jenatsch and B. Ruhstaller, *Sci. Technol. Adv. Mater.*, 2018, **19**, 291-316.
5. G. Juska, K. Arlauskas, M. Viliunas and J. Kocka, *Phys. Rev. Lett.*, 2000, **84**, 4946-4949.
6. A. J. Mozer, N. S. Sariciftci, L. Lutsen, D. Vanderzande, R. Osterbacka, M. Westerling and G. Juska, *Appl. Phys. Lett.*, 2005, **86**, 112104.
7. A. Baumann, J. Lorrmann, D. Rauh, C. Deibel and V. Dyakonov, *Adv. Mater.*, 2012, **24**, 4381-4386.
8. X. Zhao, J. Chen and N.-G. Park, *Sol. RRL*, 2019, **3**, 1800339.
9. S. Wheeler, D. Bryant, J. Troughton, T. Kirchartz, T. Watson, J. Nelson and J. R. Durrant, *The Journal of Physical Chemistry C*, 2017, **121**, 13496-13506.
10. X. Li, C.-C. Chen, M. Cai, X. Hua, F. Xie, X. Liu, J. Hua, Y.-T. Long, H. Tian and L. Han, 2018, **8**, 1800715.
11. A. H. Ip, S. M. Thon, S. Hoogland, O. Voznyy, D. Zhitomirsky, R. Debnath, L. Levina, L. R. Rollny, G. H. Carey, A. Fischer, K. W. Kemp, I. J. Kramer, Z. Ning, A. J. Labelle, K. W. Chou, A. Amassian and E. H. Sargent, *Nat. Nanotechnol.*, 2012, **7**, 577-582.
12. S. Ameen, M. S. Akhtar, H.-K. Seo, M. K. Nazeeruddin and H.-S. Shin, *J. Phys. Chem. C*, 2015, **119**, 10379-10390.